Photoinduced transient spectroscopy of defect centers in GaN and SiC

© P. Kamiński¶, R. Kozłowski, M. Kozubal, J. Żelazko, M. Miczuga*, M. Pawłowski*

Institute of Electronic Materials Technology,
01-919 Warszawa, Poland
* Military University of Technology,
00-908 Warszawa, Poland

(Получена 12 сентября 2006 г. Принята к печати 3 октября 2006 г.)

The potentialities of photoinduced transient spectroscopy in terms of investigation of defect centers in wide band gap semiconductors are presented. The experimental system dedicated to measurements of the photocurrent transients at temperatures 20–800 K is described and a new approach to extraction of trap parameters from the photocurrent relaxation waveforms recorded in a selected temperature range is presented. The approach is based on the two-dimensional analysis of the waveforms as a function of time and temperature using the correlation procedure. As a result, the three-dimensional images showing the temperature changes of the emission rate for detected defect centers are produced and a neural network method is applied to determine the parameters of defect centers. The new approach is exemplified by studies of defect centers in high-resistivity GaN : Mg and semi-insulating 6*H*-SiC : V.

PACS: 71.55.Eq, 71.55.Ht, 72.40.+w

1. Introduction

Quality assessment of epitaxial GaN and semi-insulating (SI) SiC wafers is of great importance in terms of manufacturing advanced monolithic microwave integrated circuits (MMICs) operating at millimeter-wave frequencies. In particular, the development of broadband satellite communication systems has involved a substantial demand for high-quality power devices based on these materials. The power densities recorded for GaN-based high-electron mobility transistors (HEMTs) at 10−100 GHz are far superior to those for GaAs HEMTs. The technology allowing to achieve the best device performance today is to grow GaN HEMT structures on wafers made from SI SiC. This is because of the excellent thermal conductivity and smaller lattice mismatch of SiC compared to sapphire substrate. Semi-insulating SiC substrates are required in order to reduce connection capacitance and dielectric losses.

The objective of this paper is to show the potentialities of the photoinduced transient spectroscopy (PITS) as a powerful tool for investigation of defect levels in wide band gap semiconductors with high resistivity. A new approach to visualization of the measurement results is presented. It is based on creating the images of spectral fringes depicting the temperature dependences of the emission rate of charge carriers for detected defect centers. For this purpose, a two-dimensional analysis of the temperature-induced changes in the photocurrent relaxation waveforms is performed and the fringes are obtained through projecting the spectral surfaces on the plane given by the axes for the temperature and the emission rate. The improved PITS technique is applied to investigation of defect centers in epitaxial highly compensated GaN : Mg and bulk SI SiC : V. Magnesium ($3s^2$) is a shallow dopant used in GaN to produce *p*-type conductivity. However, it easily forms complexes with native defects and residual impurities introducing deep levels in the band gap [1–4]. So, the defect structure of GaN : Mg is fairly complicated and so far has not been fully characterized. Vanadium ($3d^3 4s^2$) is an amphoteric impurity in SiC and acts as a deep acceptor or a deep donor compensating shallow level impurities such as residual nitrogen and boron [5–10]. Vanadium atoms may also bind to other impurities or intrinsic defects producing complex defects whose electronic properties still remain unknown [5–10].

¶ E-mail: pawel.kaminski@itme.edu.pl
Fax: (+48 22)8645496

2. Experimental details

The Mg-doped epitaxial GaN used in this work was grown on (0001) sapphire substrate by metal-organic chemical vapour deposition (MOCVD). The thickness of the epitaxial layer was 0.5 μm. The material was not subjected to the post-growth annealing, usually used to activate *p*-type conductivity, so its resistivity at room temperature was $2.0 \cdot 10^4\ \Omega \cdot$ cm. The activation energy, determined from the temperature dependence of dark current (TDDC), was 0.185 eV. The wafer of V-doped SI 6*H*-SiC was cut out perpendicularly to the *c* axis ($\langle 0001 \rangle$ direction) from a bulk crystal grown by physical vapour transport method (PVT). The both sides of the wafer, whose thickness was 388 μm, were mechano-chemically polished. The (0001) Si-face surface was prepared accordingly to the requirements for epitaxial substrates and the backside was of optical quality. The wafer resistivity at room temperature was $1.0 \cdot 10^{10}\ \Omega \cdot$ cm and the activation energy of dark conductivity was equal to 1.26 eV.

For PITS measurements, arrays of Pt ohmic contact pairs were deposited on the surface of the samples of the both materials. The width of the region between two co-planar contacts was 0.7 mm. The samples were cut into chips of $4 \cdot 9\ \text{mm}^2$ in area, which were mounted in the sample holder of a cryostat or vacuum chamber

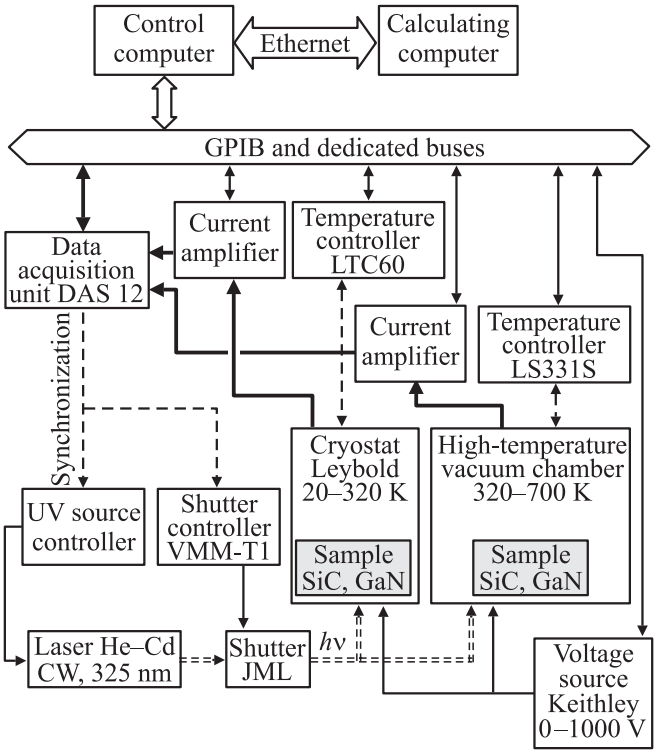

Figure 1. Experimental system for studying defect centers in wide band gap semiconductors by photoinduced transient spectroscopy.

dedicated to measurements at temperatures ranging from 320 to 800 K. The schematic illustration of the experimental setup used for characterization of defect centers in high-resistivity GaN : Mg and SI SiC : V is shown in Fig. 1. The measurements of photocurrent transients are carried out in the temperature range of 20–800 K with steps ranging from 1 to 10 K. The excess charge carriers are generated by means of a He–Cd laser continuously emitting ultraviolet (UV) radiation with the wavelength of 325 nm (3.82 eV) and power of 40 mW. The photon flux can be changed in the range $10^{16}-10^{18}\,\mathrm{cm}^{-2}\cdot\mathrm{s}^{-1}$ by means of a set of optical filters. The UV pulses are shaped by a mechanical shutter with electronic triggering. The width of these pulses can be varied from 10 ms to 20 s and the period between them can be changed from 50 ms to 100 s. The voltage between two co-planar contacts is usually in the range of 1–40 V. The photocurrent transients are amplified using a Keithley 428 fast current amplifier (conductance–voltage converter) and then digitized with a 12-bit amplitude resolution and a 1-μs time resolution. In order to improve the signal-to-noise ratio the digital data are averaged usually taking $50-500$ waveforms. For further processing each photocurrent relaxation waveform is normalized with respect to the photocurrent amplitude at the end of the UV pulse. Since the time constant of the shutter operation is limited to 0.1 ms, the shorter temperature-induced changes in the relaxation waveforms can not be recorded. In other words, the maximum value of the emission rate window is $\sim 10^4\,\mathrm{s}^{-1}$.

According to the models dealing with the PITS technique [11,12], the photocurrent relaxation measured after switching-off the excitation pulse is related to the thermal emission of charge carriers when the following conditions are fulfilled: retrapping of the carriers by the centers is neglected, the time constant of the relaxation waveform is much longer than the carrier lifetime ($\tau_{\mathrm{rel}} \gg \tau_n$) and the temperature dependence of the reciprocal of the relaxation waveform time constant follows the Arrhenius formula. These conditions are met in our experiment, for the time constant changes in the range from 1 to 10^{-4} s and the values of carrier lifetime in GaN and SiC reported in [13,14] are $10^{-7}-10^{-8}$ s. Taking into account the above-mentioned conditions, we can assume that the time constant of the photocurrent relaxation waveform is equal to the reciprocal of the emission rate. So, the parameters of defect centers can be determined derectly from the temperature dependence of the emission rate fitted with the Arrhenius formula. However, the amplitude of the waveform is proportional to the mobility–lifetime product ($\mu\tau$), as well as to the emission rate, which are dependent on temperature. Therefore, the photocurrent relaxation waveform, recorded at a given temperature, is normalized with respect to the photocurrent amplitude at the end of the excitation (UV) pulse.

In order to obtain the images of spectral fringes, the two-dimensional analysis of the photocurrent relaxation waveforms recorded in a range of temperatures is performed using the correlation procedure [15,16]. As a result, the experimental data are transformed into the spectral surface visualized in the three-dimensional (3D) space as a function of two variables: the temperature (T) and the emission rate (e_T). The processes of thermal emission of charge carriers from detected detect levels manifest themselves as the folds on the spectral surface, and the projections of these folds on the plane determined by the axes (T, e_T) give the experimental spectral fringes. To extract the parameters of defect centers, the ridgeline of each fold is found and also projected on the plane in the domain of the temperature and emission rate. Next, the projected line, which gives the temperature dependence of emission rate for the particular defect center, is fitted with the Arrhenius formula [16]

$$e_T(T) = AT^2 \exp(-E_a/k_B T), \qquad (1)$$

where e_T is the thermal emission rate of electrons or holes, E_a is the activation energy, k_B is the Boltzmann constant and $A = \gamma\sigma$ is the product of the material constant γ and the apparent capture cross-section σ for electrons or holes. As a result, the activation energy E_a and the pre-exponential factor A, related to the capture cross-section, are calculated. The ridgeline of the fold in the two-dimensional spectrum and the parameters of the defect center are determined by means of a neural network (NN) [15,17]. The neural approximator has the form of two-layered perceptron whose inputs represent the variables in the approximating function The activation function of hidden neurons is assumed as a weighted sum of two sigmoid functions. Thus, each hidden neuron can model the lateral surface of the fold in the two-dimensional spectrum. When added together, they create

the approximating surface that morphologically matches the shape of the fold corresponding to the defect center.

3. Results

3.1. Images of spectral fringes for high-resistivity GaN : Mg

The images of spectral fringes obtained by the two-dimensional analysis of the photocurrent ralaxation waveforms recorded in four temperature regions for high-resistivity GaN : Mg are illustrated in Figs 2 and 3. In the temperature range of 170–200 K two fringes corresponding to defect centers TS1 (0.126 eV) and TS2 (0.122 eV) are observed. The parameters of these centers are consistent with those determined for magnesium acceptor (Mg_{Ga}) from the Hall measurements [3], as well as from the studies preformed by the current deep level transient spectroscopy [1]. It should by noted that the reported values of the Mg_{Ga} acceptor activation energy are in the range of 0.1–0.15 eV [1–3]. The occurrence of two levels related to the Mg_{Ga} acceptor can be explained by taking into account a high dislocation density in GaN epitaxial layers deposited on sapphire substrates by MOCVD technique. Thus, it can be assumed that the traps TS1 (0.126 eV) and TS2 (0.122 eV) are the hole traps related to the Mg dopant atoms located in different regions of the epitaxial layer. So, the trap TS2 (0.122 eV) is presumably associated with the Mg atoms occupying gallium sites in the vicinity of dislocations and being affected by the high electric and strain fields. On the other hand, the trap TS1 (0.126 eV) can be attributed to the Mg atoms located in the dislocation-free regions. It should be added that the activation energy of dark conductivity (0.185 eV) is significantly higher than the activation energies

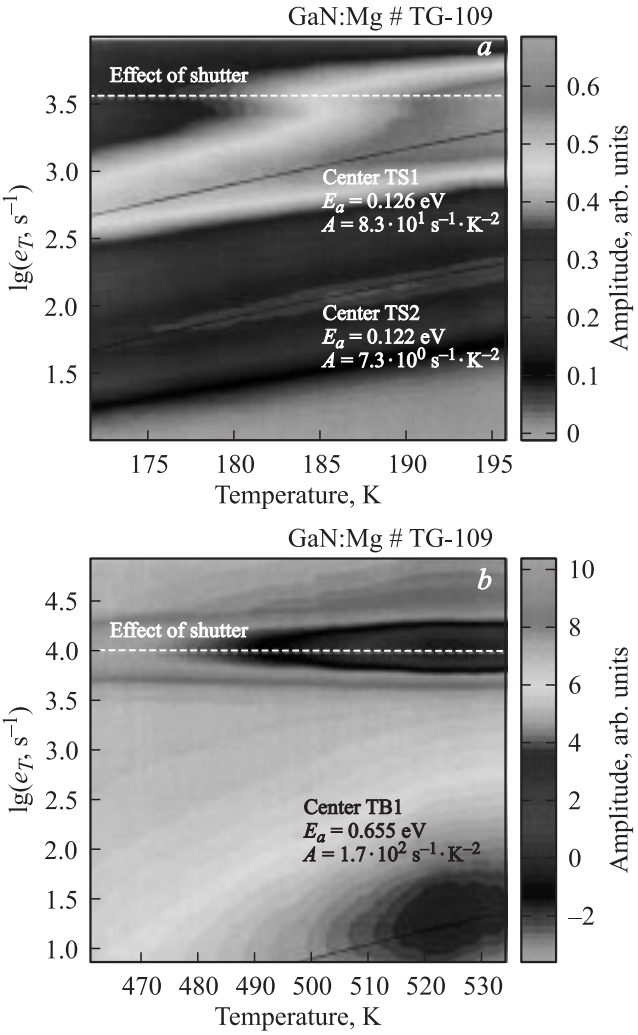

Figure 2. Images of spectral fringes obtained by the two-dimensional analysis of the photocurrent relaxation waveforms recorded in two temperature ranges 170–200 K (a) and 470–530 K (b) for the sample of high-resistivity GaN : Mg. The solid lines illustrate the temperature dependences of emission rate e_T for detected defect centers.

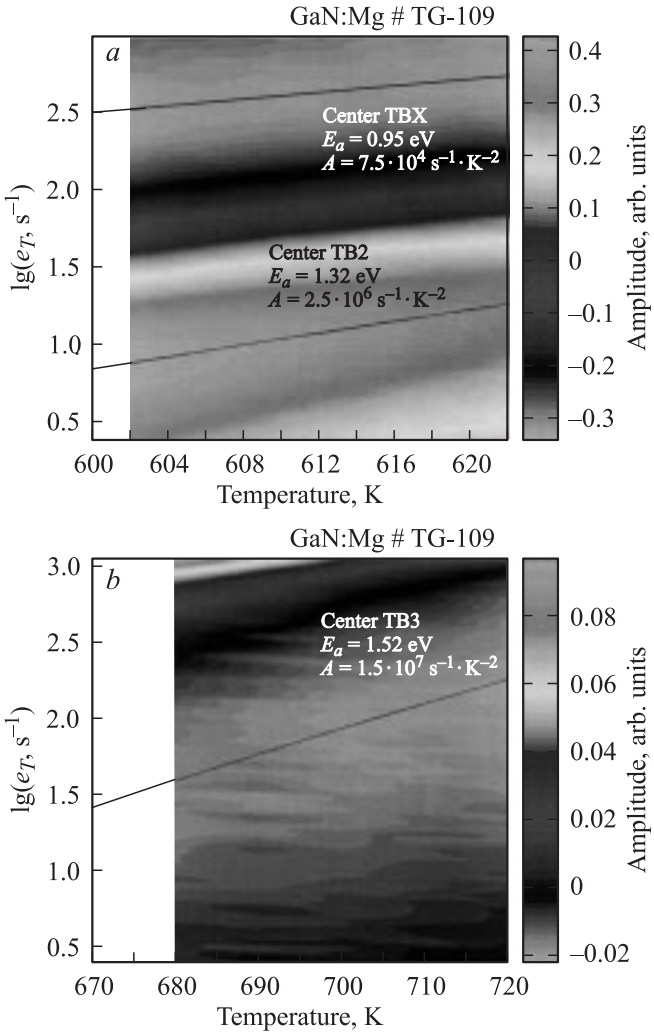

Figure 3. Images of spectral fringes obtained by the two-dimensional analysis of the photocurrent relaxation waveforms recorded in two temperature ranges 600–620 K (a) and 680–720 K (b) for the sample of high-resistivity GaN : Mg. The solid lines illustrate the temperature dependences of emission rate e_T for detected defect centers.

Table 1. Summary of parameters of defect centers detected by the PITS method in high-resistivity epitaxial GaN : Mg

Trap label	Activation energy E_a, eV	Pre-exponential factor A, $s^{-1} \cdot K^{-2}$	Tentative identification
TS1	0.126	$8.3 \cdot 10^1$	h, acceptor, Mg_{Ga} [1,3]
TS2	0.122	7.3	h, acceptor, Mg_{Ga} in vicinity of dislocations [1,3]
TB1	0.655	$1.7 \cdot 10^2$	e, Mg acceptor–nitrogen vacancy complex (Mg_{Ga}–V_N) [3,4]
TBX	0.950	$7.5 \cdot 10^4$	e, donor, gallium vacancy–nitrogen interstitial complex ($V_{Ga}-N_i$) [20]
TB2	1.32	$2.5 \cdot 10^6$	new trap
TB3	1.52	$1.5 \cdot 10^7$	new trap

Note. e or h denotes electron or hole trap, respectively.

of traps TS1 (0.126 eV) and TS2 (0.122 eV). This indicates that the Fermi level position extrapolated to 0 K is not pinned to the Mg level since the Mg acceptors are likely to be compensated with shallow (residual silicon) and deep donors. The substantial changes of the dark current with temperature were observed above 500 K.

In the temperature range of 470–530 K only one broad spectral fringe corresponding to the center TB1 (0.655 eV) is observed. It worth noting, that this fringe was obtained by the two-dimensional analysis of the photocurrent relaxation waveforms with the negative amplitudes. In other words, the change in the occupancy of traps induced by the UV pulse resulted in lowering the conductivity compared to the equilibrium value. So, the fringe related to the deep center TB1 (0.655 eV) was obtained by the projection of the hollow occurring on the spectral surface due to negative amplitudes of the photocurrent relaxation waveforms. The mechanism responsible for the occurrence of the negative amplitude of the photocurrent relaxation waveforms has not been until now fully understood. However, there are some results, obtained either experimentally [11,18] or by simulation [19], allowing for an explanation of this phenomenon. They indicate that the negative amplitude of the relaxation waveform can result from the specific change in the occupancy of a deep level involved in the material compensation. This seems to be the case when deep donor or acceptor centers influencing the material conductivity are in excess filled with majority charge carriers. For example, the negative amplitude of the photocurrent relaxation waveform is observed when deep donor EL2 centers are filled with electrons in n-type high-purity semi-insulating GaAs, as well as when deep Fe-related acceptor centers are filled with electrons in n-type high-purity semi-insulating InP. So, similarly as in the capacitance spectroscopy, the amplitude of the photocurrent relaxation waveform can be positive, when the deep traps are filled with the minority carriers, or negative when the traps are filled with the majority carriers. It should be added, however, that in the PITS experiments compensated materials are used and in many cases it is difficult to establish whether the conductivity is of n- or p-type. The sample of high-resistivity, non-activated GaN : Mg seems to be n-type and the photocurrent relaxation waveforms with the negative amplitudes are likely to be related to the thermal emission of electrons from deep centers.

Taking into account the results reported in [3], the center TB1 (0.655 eV) can be assigned to a complex defect composed of the magnesium acceptor and nitrogen vacancy ($Mg_{Ga}-V_N$). According to the results obtained by the positron annihilation method [4], $Mg_{Ga}-V_N$ complexes compensate isolated Mg_{Ga} acceptors and are responsible for the high resistivity of non-activated GaN : Mg. Annealing at the temperatures 500–800°C leads to decomposition of these complexes and activation of the p-type conductivity. In the temperature range of 600–620 K two distinctive spectral fringes are seen. It should be added, however, that the fringe at higher emission rates, corresponding to the center TBX (0.95 eV) represents the hollow on the spectral surface, whereas the fringe at lower emission rates, corresponding to the center TB2 (1.32 eV) represents the fold on the spectral surface. In view the results reported in [20], the center TBX (0.95 eV) can be identified with an electron trap $E_c-0.96$ eV attributed to the complex involving gallium vacancy and nitrogen interstitial ($V_{Ga}-N_i$). The identification of the center TB2 (1.32 eV) is difficult because of the shortage of experimental data dealing with midgap centers in GaN. The fringe observed in the temperature range 680–720 K is due to thermal emission of charge carriers from the center TB3 (1.52 eV). This fringe represents the hollow on the spectral surface resulting from negative amplitudes of the photocurrent relaxation waveforms. It should be added, that the intensity of this fringe is much lower compared to the fringes shown in Figs 2, *a, b* and 3, *a*. So, it is not related to doping with magnesium but it is likely to be conditioned by native defects or complex involving native defects or residual impurities.

The parameters of defect centers detected by the PITS measurements in high-resistivity GaN : Mg are summarized in Table 1.

The results obtained indicate that non-activated GaN : Mg is a highly compensated material due to the presence of deep donors related to complexes formed by the magnesium acceptors with nitrogen vacancies and by the nitrogen interstitials with gallium vacancies. The nitrogen interstitials are likely to be produced during the epitaxial growth due to the high ratio (~ 1000) of the nitrogen atom concentration to the gallium atom concentration in the gas phase. The high concentration of nitrogen vacancies presumably results from the high density of dislocations, which are generated in

consequence of the lattice mismatch between the epitaxial layer and the sapphire substrate.

3.2. Images of spectral fringes for SI 6*H*-SiC : V

The images of spectral fringes obtained by the two-dimensional analysis of the photocurrent relaxation waveforms recorded in four temperature ranges for semi-insulating 6*H*-SiC : V are presented in Figs 4 and 5. The fringe shown in Fig. 4, *a*, observed in the range 40–70 K, is due to the thermal emission of charge carriers from the center TV1 whose activation energy is 0.08 eV. It should be noted that the emission rate is in the range of $10^3-10^4\,s^{-1}$ and the upper part of this fringe is affected by the limited speed of the shutter operation. In view of the results reported in [6–8], the shallow center TV1 (0.08 eV) can by assigned to a residual nitrogen atom in a hexagonal site. The distinct fringe shown in Fig. 4, *b*, observed in the range 160–250 K, is related to the center TV2 (0.28 eV). It is seen that in the temperature range 220–250 K the emission rate of charge carriers is around $10^4\,s^{-1}$, so the shape of this fringe is also affected by the shutter. According to the results reported in [8], the center TV2 (0.28 eV) is likely to be attributed to the boron acceptor. Fig. 5, *a* illustrates two fringes, observed in the temperature range 300–315 K, associated with the centers TV3 (0.43 eV) and TV4 (0.78 eV). The experimental data reported in [10] indicate, that the former can be tentatively identified with an electron trap $E_c-0.44$ eV occurring in neutron-irradiated *n*-type 6*H*-SiC and assigned to a complex formed by a vanadium atom and a native defect. In view of the results presented in [5–7], the latter is likely to be the vanadium acceptor $V^{3+/4+}$. So, the fringe corresponding in Fig. 5, *a* to the center TV4 (0.78 eV) is due to thermal emission of electrons from vanadium acceptors. Fig. 5, *b* shows the fringe corresponding to the deep center

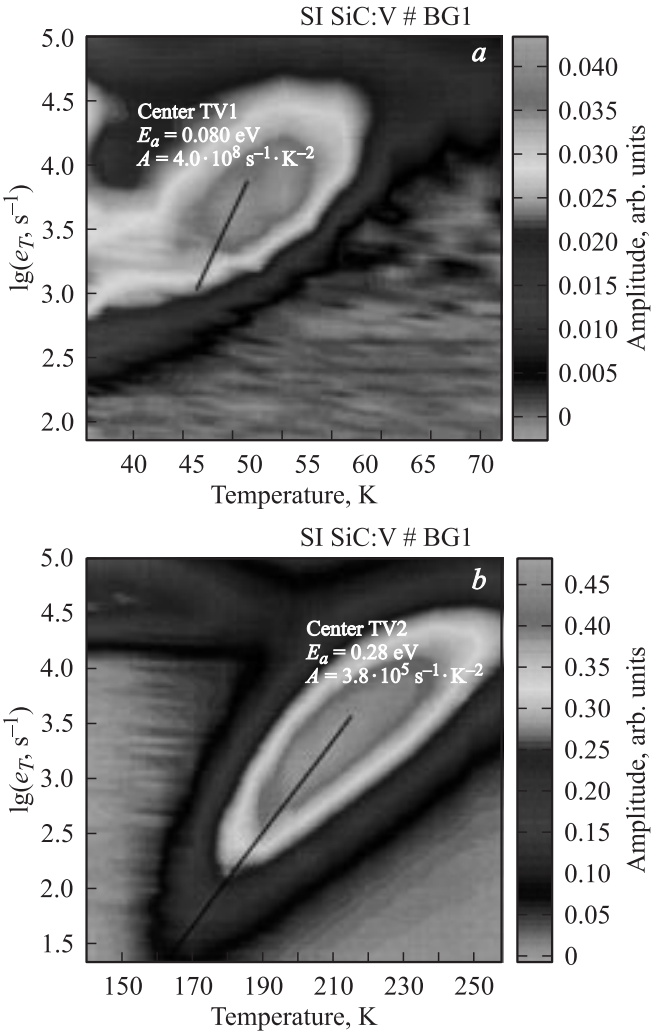

Figure 4. Images of spectral fringes obtained by the two-dimensional analysis of the photocurrent relaxation waveforms recorded in two temperature ranges 40–70 K (*a*) and 160–250 K (*b*) for the sample of SI 6*H*-SiC : V. The solid lines illustrate the temperature dependences of emission rate e_T for detected defect centers.

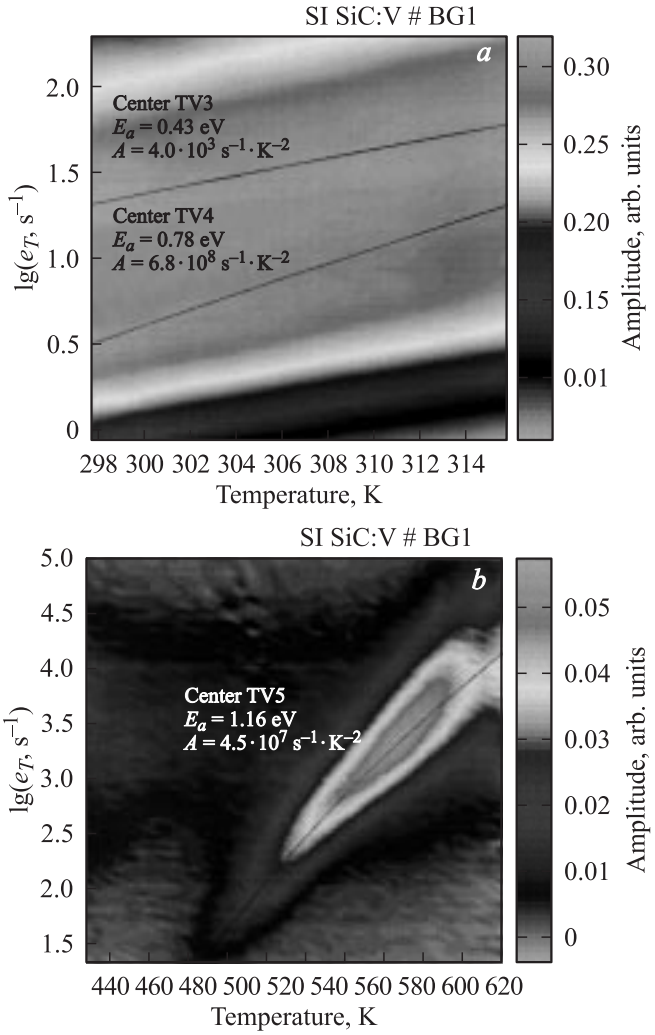

Figure 5. Images of spectral fringes obtained by the two-dimensional analysis of the photocurrent relaxation waveforms recorded in two temperature ranges 300–315 K (*a*) and 500–600 K (*b*) for the sample of SI 6*H*-SiC : V. The solid lines illustrate the temperature dependences of emission rate e_T for detected defect centers.

Table 2. Summary of parameters of defect centers detected by the PITS method in SI 6*H*-SiC : V

Trap label	Activation energy E_a, eV	Pre-exponential factor A, $s^{-1} \cdot K^{-2}$	Tentative identification
TV1	0.08	$4.0 \cdot 10^8$	*e*, donor, N_C in hexagonal site [6–8]
TV2	0.28	$3.0 \cdot 10^5$	*h*, acceptor, B_{Si} [8]
TV3	0.43	$4.0 \cdot 10^3$	*e*, NE1, $E_c - 0.44$ eV [10]
TV4	0.78	$6.0 \cdot 10^8$	*e*, acceptor, $V^{3+/4+}(3d^2/3d^1)$ [5–7]
TV5	1.16	$4.5 \cdot 10^7$	*h*, donor, $V^{5+/4+}(3d^0/3d^1)$ [5–7]

Note. *e* or *h* denotes electron or hole trap, respectively.

TV5 (1.16 eV). The thermal emission of charge carriers from this center is observed at the temperatures 500–600 K. The experimental data obtained so far indicate [5–7] that the center TV5 (1.16 eV) can be assigned to the vanadium donor level $V^{5+/4+}$.

The parameters of defect centers detected by the PITS measurements in semi-insulating 6*H*-SiC : V are summarized in Table 2.

According to the results obtained, the semi-insulating properties of vanadium doped 6*H*-SiC are achieved through the compensation of shallow nitrogen donors with vanadium deep acceptors, as well as through the compensation shallow boron acceptors with vanadium deep donors. Thus, the amphoteric properties of vanadium dopant allow for the change of SiC resistivity in a very broad range, far above $10^{10}\ \Omega \cdot$ cm. Moreover, the material resistivity can be controlled both by the boron and vanadium concentrations.

4. Conclusion

A new approach to extraction of defect center parameters by the two-dimensional analysis of the temperature-induced changes in the photocurrent relaxation waveforms is presented. Advantages of the PITS technique with implementation of this approach are exemplified by studies of defect centers in high-resistivity epitaxial GaN : Mg and bulk SI 6*H*-Si : V. The charge compensation of Mg acceptors in non-annealed GaN : Mg is found to be mainly due to deep levels located at $E_c - 0.655$ eV and $E_c - 0.95$ eV attributed to magnesium–nitrogen vacancy complex ($Mg_{Ga} - V_N$) and Ga vacancy–nitrogen interstitial complex (V_{Ga}–N_i), respectively. The material properties can be also affected by midgap levels with activation energies of 1.32 and 1.52 eV. The semi-insulating properties of 6*H*-SiC : V are due to the compensation of residual nitrogen donors with vanadium acceptors, introducing the deep level at $E_c - 0.78$ eV, as well as due to the compensation of boron acceptors with vanadium donors, characterized by the deep level at $E_v + 1.16$ eV.

The work was supported in part by the Polish Ministry of Science and Higher Education under Grant No. 3 T10C 028 30 and by the ITME Research Fund (Project No. 14-1-1023-5). We thank Dr Elżbieta Litwin-Staszewska of Unipress for providing GaN samples for this work.

References

[1] Y. Nakano, T. Kachi. Appl. Phys. Lett., **79**, 1631 (2001).
[2] R. Piotrzkowski, E. Litwin-Staszewska, T. Suski, I. Grzegory. Physica B, **308–310**, 47 (2001).
[3] E. Litwin-Staszewska, T. Suski, R. Piotrzkowski, I. Grzegory, J.L. Robert, L. Kończewicz, D. Wasik, E. Kamińska, D. Cote, B. Clerjaud. J. Appl. Phys., **89**, 7960 (2001).
[4] S. Hautakangas, J. Oila, M. Alatalo, K. Saarinen. L. Liszkay, D. Seghier, H.P. Gislason. Phys. Rev. Lett., **90**, 137 402 (2003).
[5] M.E. Zvanut, V.V. Konovalov, H. Wang, W.C. Mitchel, W.D. Mitchell, G. Landis. J. Appl. Phys., **96**, 5484 (2004).
[6] J.R. Jenny, J. Skowronski, W.C. Mitchell, H.M. Hobgood, R.C. Glass, G. Augustine, R.H. Hopkins. Appl. Phys. Lett., **68**, 1963 (1996).
[7] W.C. Mitchel, W.D. Mitchell, H.E. Smith, M.E. Zvanut, W. Lee. Mater. Res. Soc. Symp. Proc., **911**, B05 (2006).
[8] O. Evwaraye, S.R. Smith, W.C. Mitchel, H.McD. Hobgood. Appl. Phys. Lett., **71**, 1186 (1997).
[9] S.W. Huh, H.J. Chung, S. Nigam, A.Y. Polyakov, Q. Li, M. Skowronski, E.R. Glaser, W.E. Carlos, B.V. Shanabrook, M.A. Fanton, N.B. Smirnov. J. Appl. Phys., **99**, 013 508 (2006).
[10] X.D. Chen, S. Fung, C.C. Ling, C.D. Beling, M. Gong. J. Appl. Phys., **94**, 3004 (2003).
[11] M.J. Brasil, P. Motisuke. J. Appl. Phys., **68**, 3370 (1990).
[12] C. Balland, J.P. Zielinger, M. Tapiero, J.G. Gross, C. Noguet. J. Phys. D: Appl. Phys., **19**, 71 (1986).
[13] R.S. Qhalid Fareed, J.P. Zhang, R. Gaska, G. Tamulaitis, J. Mickevicius, R. Aleksiejunas, M.S. Shur, M.A. Khan. Phys. Status Solidi, C **2**, 2095 (2005).
[14] G. Tamulaitis, I. Yilmaz, M.S. Shur, T. Anderson, R. Gaska. Appl. Phys. Lett., **84**, 335 (2004).
[15] M. Pawłowski, P. Kamiński, R. Kozłowski, S. Jankowski, M. Wierzbowski. Metrology and Measurement Systems, XII, 207 (2005).
[16] M. Pawłowski. Sol. St. Electron., **46**, 1879 (2002).
[17] S. Jankowski, M. Wierzbowski, P. Kamiński, M. Pawłowski. Int. J. Mod. Phys. B, **16**, 4449 (2002).
[18] R. Kozłowski, P. Kaminski, E. Nossarzewska-Orlowska, E. Fretwurst, G. Lindstroem, M. Pawłowski. Nucl. Instr. Meth. A, **552**, 71 (2005).
[19] H. Kimura, T. Kurosu, Y. Akiba, M. Iida. Jap. J. Appl. Phys., **32**, 741 (1993).
[20] M. Asghar, P. Muret, B. Beaumont, P. Gibart. Mater. Sci. Eng. B, **113**, 248 (2004).

Редактор Л.В. Шаронова